Available online at www.sciencedirect.com
ScienceDirect
Journal of the European Ceramic Society 30 (2010) 3283–3289
www.elsevier.com/locate/jeurceramsoc

Fabrication of inner complex ceramic parts by selective laser gelling

Fwu-Hsing Liu [a], Yunn-Shiuan Liao [b,*]

[a] Dept. of Mechanical Engineering, Lunghwa University of Sci. and Technol., Taiwan, ROC
[b] Dept. of Mechanical Engineering, National Taiwan University, Taipei, Taiwan, ROC

Received 16 October 2009; received in revised form 29 July 2010; accepted 2 August 2010
Available online 1 September 2010

Abstract

Various raw materials have been used in rapid prototyping (RP) technologies. However, the ceramics were seldom adopted in RP process. None of the ceramic RP processes investigates in detail the formability procedure from a single line, a single layer, to multi-layers. In this paper, a method, selective laser gelling (SLG), for generating SiO_2 parts with an overhang structure was proposed and a method of formability for affecting the dimensional accuracy and surface finish of the part was presented. A strategy was also proposed for generating pillared support to reduce a sagged deflection of the overhang and to demonstrate the ability for forming a complex-shaped part with inner channel structure. The effects of process parameters on the dimensional accuracy and surface roughness of the gelled parts were explored and a set of appropriate parameters was obtained.

Keywords: Rapid prototyping; Forming; Gelling; Ceramic; Suspension

1. Introduction

Rapid prototyping (RP) technologies employ various materials to form solid parts. For example, ultraviolet (UV) resin is used in stereolithography apparatus (SLA), metal powder is used in selective laser sintering, plastic material is used in fused deposition modeling (FDM), TZP ceramic suspensions are used in direct inkjet printing (DIP), paper sheet is used in laminated object manufacturing (LOM), and ceramic powder is used in selective laser curing (SLC).[1–6] In addition, a number of other materials have also been developed until now.

The research of RP now is focused on metal and ceramic materials due to their industrial applications.[7] Several works on metal RP have been conducted in recent years. For example, Liou developed a multi-axis laser aided manufacturing process for rapid tooling (RT); a high-speed photocopier to produce 3D objects from metal powders had been developed by Van Der Eijk.[8,9] The study on ceramics has been very rare in the literature. Fuh et al. built a silica casting mould via direct laser sintering,[7] Song researched the RP manufacturing of silica sand patterns using selective laser sintering (SLS).[10] Evans studied a solvent-based extrusion solid freeforming technology to build complex ceramic 3D structures.[11] In addition, the process of laser microsintering could directly build microceramic parts without postprocesses.[2] Moreover, a combination of mould shape deposition manufacturing (Mould SDM) and the gelcasting process was applied to fabricate ceramic heat exchangers.[12]

Only a few studies discuss the detailed building process for forming the inner complex ceramic parts. Therefore, this paper presents a method, selective laser gelling (SLG), to obtain a ceramic part with interconnected reticular porous by using an experimental method. This work explores the development of the formability for a ceramic part and explains a layer-additive process for forming a reticular 3D ceramic part overhanging from the support structure.

2. Materials and methods

2.1. Materials

The strength and accuracy are the main desired properties for manufacturing RP parts. However, the liquid-based of PR processes have greater accuracy but lack in strength; the powder-based PR possesses have better strength but less accuracy. In order to obtain higher accuracy and strength, we adopt the ceramic slurry as row materials. The slurry-based material can increase the accuracy due to the fluidity of slurries and enhance

* Corresponding author. Tel.: +886 2 2362 6431.
E-mail address: liaoys@ntu.edu.tw (Y.-S. Liao).

0955-2219/$ – see front matter © 2010 Elsevier Ltd. All rights reserved.
doi:10.1016/j.jeurceramsoc.2010.08.001

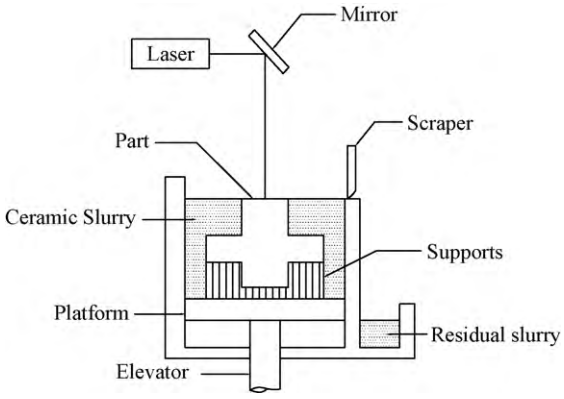

Fig. 1. Schematic diagrams of the experimental set-up.

the strength due to the hardness of ceramic after gelling process. The composition of the slurries employed herein is mixed by the silica powder with an average particle size of 25 μm in a broad distribution range and a silica sol with about 50 nm particle diameters as a binder in a proportion of 55–45 wt.%. The silica sol is obtained from Nissan Chemical Industries Ltd., Japan. The SiO_2 solid content in the sol is 40 wt.%. The silica powder is obtained from Chin Ching Silica Sand Co. Ltd., Taiwan. The purity of silica powder is 99.5%.

2.2. Experimental apparatus

An experimental RP apparatus developed in this work consists of a material paving system for paving a slurry layer, a CO_2 laser scan system for gelling the slurries to form a ceramic part, and a control system for administering the motions of the scraper and elevator as well as for determing the scan files, laser scan paths, laser scan speed, and laser power via a human–machine interface (HMI).[13] The experimental set-up is shown in Fig. 1.

The SLG process builds parts in layers. First, a layer of ceramic slurry is paved onto the surface of a platform. The component slice is then formed, and the slurry can be selectively scanned by a laser beam to form a layer of ceramic part. The platform lowers the part in a layer thickness, a scraper paves the next slurry layer and then the slurry is scanned by a laser again according to a slicing pattern. The procedure is repeated until the part is completed to form a 3D ceramic part. The silica sol in the slurry is evaporated using a laser radiation, the silica particles in the selectively scanned area are bonded by the gelled silica sol. In contrast, the un-gelled slurry left unscanned by the laser beam remains in the fluid state.

2.3. The process parameters

To explore the relation of the dimensional accuracy in the gelled layers, the process parameters used in SLG are shown in Fig. 2.[14] They ought to be investigated to determine the laser power P_L, laser scan speed V_S, layer thickness D_n, layer over-gel D_o, layer gelled depth D_s, hatch spacing H_s, line gelled depth L_t, line overlap L_o, and line gelled width L_b. In the present investigation, we have included these parameters to examine their effects on dimensional accuracy and surface roughness of the ceramic parts.

3. Generating experiments and results

The process of silica gelling is used to gel silica powder together to form a ceramic part. The details of formability for building a ceramic part can be expressed more clearly from a basic single line, a single layer, to multi-layers of gelled ceramic. In this way, the line overlap and the layer over-gel of the ceramic parts can be explored.

3.1. Generating a ceramic specimen

3.1.1. Single line of gelled ceramic

The basic unit of a specimen in the forming procedure is a single line of a gelled ceramic because the ceramic slurry is scanned by a CO_2 laser beam. Upon exposing the slurries with laser radiation, the moisture in the silica sol will be evaporated and then the "gelling process" occurs. Thus, the silica powders in a scanning path are bonded together in a certain depth by the gelled silica sol and then a single line ceramic is formed. For a laser power of 15 W, scan speed of 250 mm/s, and layer thickness of 0.1 mm, we obtained a single line of ceramic with a depth of 0.14 mm and a width of 0.42 mm (see Fig. 3).

The relation between the laser scan speed and the depth of a single line ceramic is shown in Fig. 4. As shown in the figure, the ceramic gelled depth increases upon decreasing the scan speed. Because the ceramic slurry absorbed more laser energy at lower scan speed, the gelled depth was deeper. As soon as the gelled depth was between 0.14 and 0.12 mm, each layer of

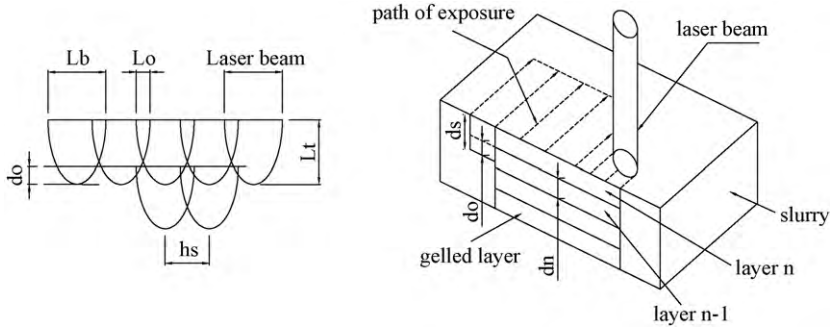

Fig. 2. Process parameters for selective laser gelling.

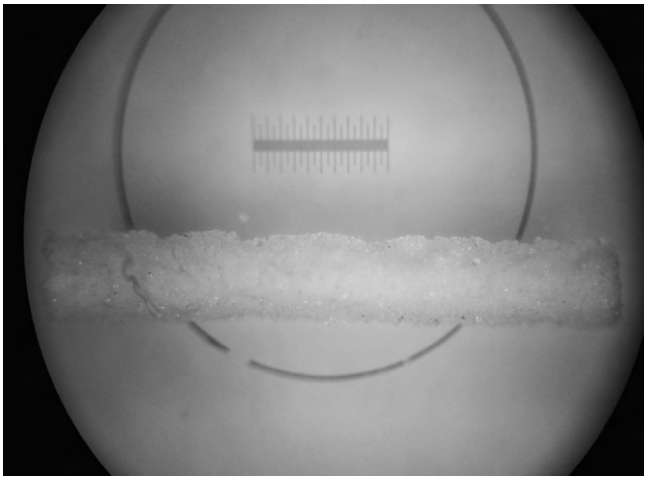

Fig. 3. A single line of a gelled ceramic.

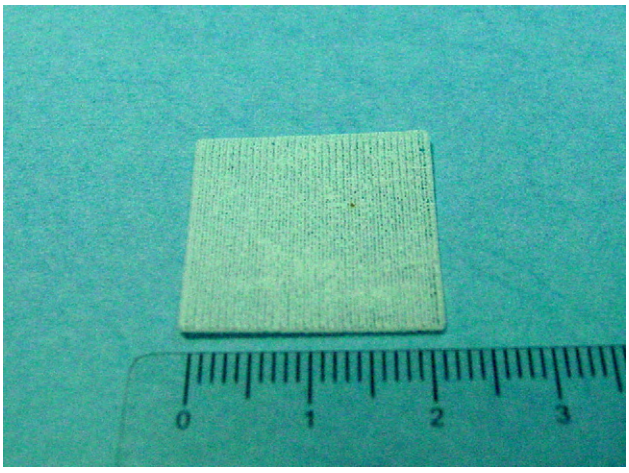

Fig. 5. A single layer of gelled ceramic.

gelled ceramic could be bonded together. That is, if the over-gel depth between layers is sufficient, e.g., the over-gel depth is in the 0.04–0.02 mm range, the silica powder can be constructed to form a ceramic layer with a definite strength, which maintains the contours of a gelled layer.

3.1.2. Single layer of gelled ceramic

As mentioned above, the generating processes for a single line ceramic are repeated to form a single layer of a gelled ceramic, which keeps a suitable overlap between the single line ceramic. In our experiments, we adjusted the laser hatch spacing to obtain an overlap between 5 and 50%. If the overlap was less than 15%, the bonded strength was insufficient to construct a single layer ceramic. In contrast, when the overlap exceeded 40%, the gelled layer yielded warping due to the laser power density being too high. Thus the formation of the gelled ceramic layer failed.

When the warp is higher than the thickness of a paving layer, the gelling layer cannot be generated because this warped portion disturbs the motion of a scraper. If the overlap of a gelled layer is varied from 20 to 30%, then the warp is kept in a smaller range to avoid scraping by a scraper. Thus a gelled layer can be successfully generated in a suitable overlap. Fig. 5 shows a single layer of gelled ceramic specimen with dimensions of 20 mm × 20 mm as the overlap is 25%.

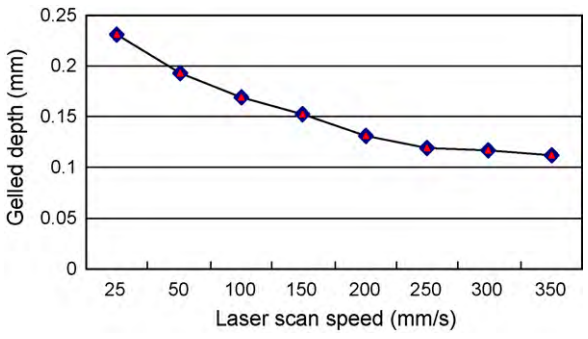

Fig. 4. The relation between laser scan speed and gelled depth.

3.1.3. Multi-layers of gelled ceramic

The above results can be applied in building multiple-layers of a gelled ceramic. As the over-gel of each layer equaled 30%, the ceramic parts had sufficient gelled strength. Neither higher nor lower over-gel was suitable for building ceramic parts. For example, when the over-gel was below 10%, the bonding strength of a ceramic body was insufficient due to the poor gelling effect among gelled layers, which caused the gelled layers to be separated.

On the other hand, when over-gel exceeded 50%, the gelled layer yielded warp that would be damaged by the scraper so that the layer could not be constructed. Therefore, the suitable process parameters were as follows: the layer thickness = 0.1 mm, over-gel = 30%, overlap = 25%, laser power = 15 W, and laser scan speed = 250 mm/s. Those data were used to generate a 3D part of multi-layers ceramic with dimensions of 20 mm × 20 mm × 8 mm as shown in Fig. 6.

3.2. The dimensional accuracy and surface roughness

In order to construct more accurate parts, the influence of process parameters on the dimensional accuracy of the parts must be explored. The dimension in the ceramic specimen shown

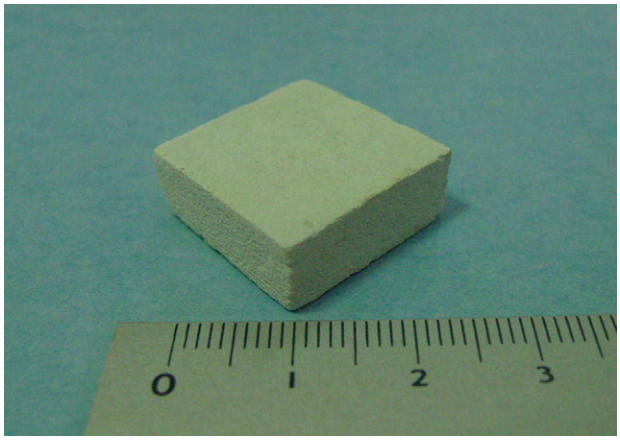

Fig. 6. A 3D ceramic part with multi-layers.

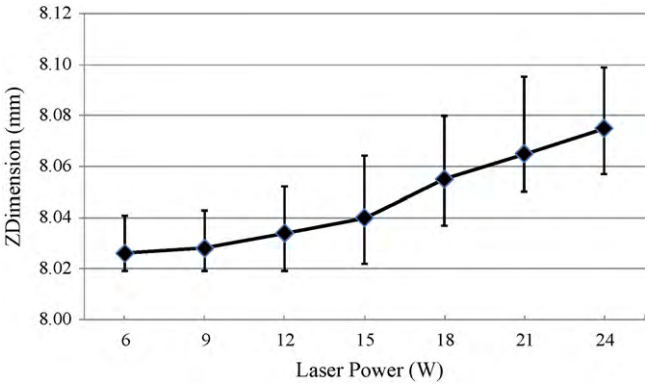

Fig. 7. The relation between the *Z*-axial dimension and laser power.

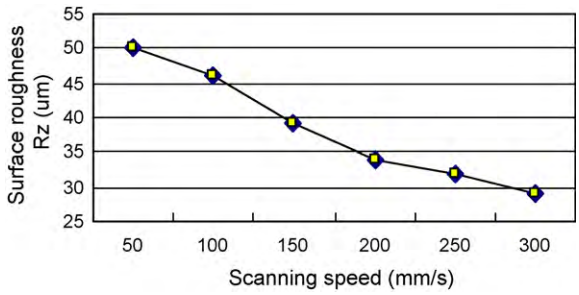

Fig. 9. The relation between laser scanning speed and surface roughness. When the laser scan speed was slower, the laser power density absorbed by specimen was larger and then the surface roughness increased due to the greater heat distortion.

in Fig. 6 was measured by a coordinated measuring machine (CMM). The relation between the *Z*-axial dimension and laser power is shown in Fig. 7. It can be seen from this figure that when the laser power exceeded 18 W, the margin of errors along the vertical direction was also increased. In contrast, the laser power below 12 W could be adopted to decrease the value of deviation. Therefore, we can obtain higher dimensional accuracy due to the less sagged deflection and a faster laser scan speed due to greater laser power if we adopt a laser power of 15 W.

The surface roughness obtained from the flank of the specimen under various laser powers at a laser scan speed of 250 mm/s is plotted in Fig. 8. The solid line represents the surface roughness in a direction parallel to the *Z*-axis and the dotted line shows the surface roughness in a direction perpendicular to the *Z*-axis. This figure shows that the surface roughness increases for a laser power of 9–24 W and decreases for a laser power of 6–9 W.

The laser power of 6 W provided just enough energy to initiate the "gelling process", but the development of gelling in silica sol was still unstable in this state. When a laser beam scaned the silica slurries, the local zone of the silica sol could not finish the gelling process due to insufficient laser power density. That is, the moisture in the slurries cannot be completely evaporated and this zone still maintains the slurry state. Hence the scanned silica powders that are gelled together form the silica aggregate cluster, but those silica powders that are un-gelled remain in the incoherent state. The surface of the specimen is pitted with aggregated cluster. For this reason, the value of surface roughness is decreased for a laser power of 6–9 W.

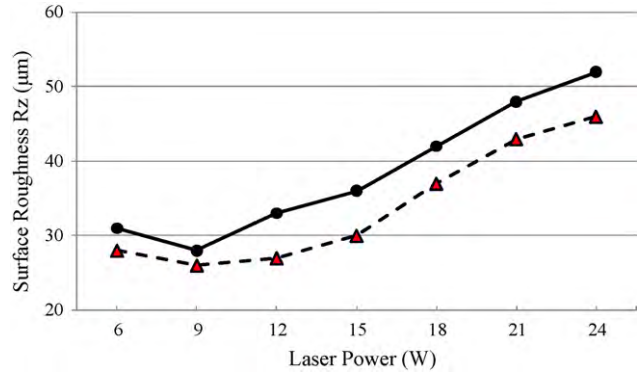

Fig. 8. The surface roughness of a ceramic part vs. laser power. The solid line represents the surface roughness in a direction parallel to the *Z*-axis and the dotted line shows the surface roughness in a direction perpendicular to the *Z*-axis.

The relation between surface roughness and laser scanning speed is shown in Fig. 9. The value of surface roughness decreases as the laser scan speed increases. When the laser scan speed was slower, the laser power density absorbed by specimen was larger and then the surface roughness increased due to the greater heat distortion. In contrast, when the laser scan speed was faster, the laser power density was smaller and then the surface roughness reduced due to less heat distortion.

3.3. The overhanging structure

The influence of an overhanging structure on dimensional accuracy is obvious besides the contours of a particular part. The direction of a warp yielded in RP parts is either upward or downward as soon as the warp occurs. The SLA and SLS processes yield an upward warp, but the SLG process yields a downward warp. To explain the influence of overhanging on SLG, we built a specimen as shown in Fig. 10(a). Various spans of the overhanging are related to the sagged deflection shown in Fig. 10(b). As shown in the figure, without additional support structure, a deflection is proportional to the span of an overhanging. The influence of deflection on the span is shown in Table 1.

As shown in Table 1, the overhanging had a deflection of 68.4 μm within a span of 2 mm, which exceeded the maximum of surface roughness (53 μm R_Z). To reduce the amount of warp and enhance the dimensional accuracy, we generated a support with a span of 1.5 mm under the overhanging. Moreover, a higher accuracy part could be obtained because the overhanging had a sagged deflection of 49.7 μm which is approximately equal to the maximum of surface roughness. Hence, the overhanging structure does not affect the dimensional accuracy of the part when the span of overhanging is less than 1.5 mm.

3.4. The support and inner channel structure

Generally speaking, the ceramic slurries having a definite of suspension are significant.[15] In this study, the silica slurries provide suspension to maintain a short overhanging with a small

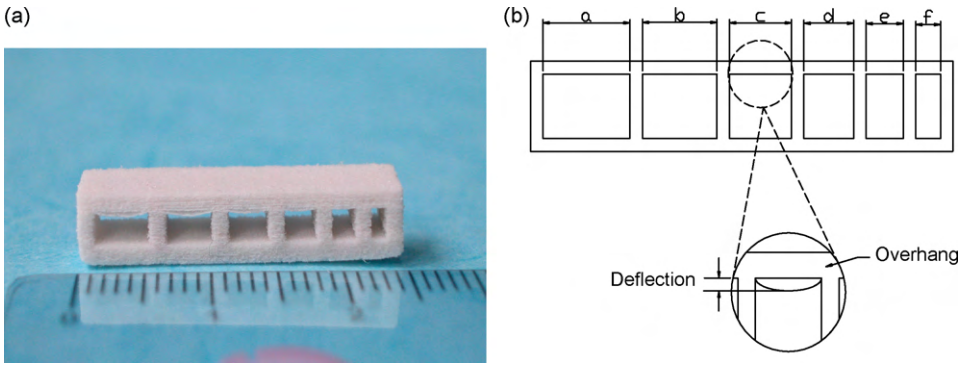

Fig. 10. A test specimen with various span and deflection. (a) A real specimen, and (b) schematic of the various spans related to the sagged deflection.

Table 1
Relation between the overhanging span and sagged deflection.

	Section					
	a	*b*	*c*	*d*	*e*	*f*
Layer thickness	0.1 mm	0.1 mm	0.1 mm	0.1 mm	0.1 mm	0.1 mm
Overhanging span	3.5 mm	3.0 mm	2.5 mm	2.0 mm	1.5 mm	1.0 mm
Span-thick rate	×35	×30	×25	×20	×15	×10
Sagged deflection	261.5 μm	218.2 μm	103.2 μm	68.4 μm	49.7 μm	35.7 μm

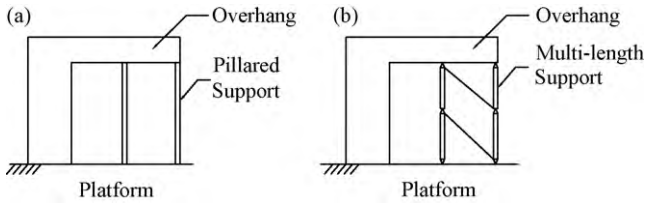

Fig. 11. Schematic diagrams of the ceramic gelled support structure. (a) The single pillared support, and (b) the multi-length of pillared support.

deflection but a support structure needs to be generated when the length of overhanging exceeds a definite distance. When the span of overhanging exceeded 2.5 mm, the deflection of the gelled layer was approximately 103.2 μm which is greater than the layer thickness, and the layer could hardly be generated. Thus a pillared support of structure can be constructed as shown in Fig. 11(a).

Although the pillared support can reduce the amount of deflection on the overhanging, two bottlenecks in this method need to be overcome. First, when the rate of height–width exceeds eight, the support can hardly be constructed because of the collapse of support. Second, both end of the pillared support can hardly be removed because the support can adhere tight to the bottom of the overhanging and the top surface of the substrate.

Therefore we propose a strategy, multi-length pillared support structure, to overcome above bottlenecks as shown in Fig. 11(b). The multi-length of a pillared support was generated below the overhanging instead of a single pillared support. Also, an added support with an inclination was constructed between the support to maintain the strength of the support and to avoid the support collapsing. The size of the joints between the supports decreased in order to easily remove the support. In addition, the joints between the overhanging and the support were also easily removed including the joints between the support and the platform. After the ceramic part was completed, the support structure and residual slurries needed to be removed via spraying water. As soon as the water is sprayed on the multi-length

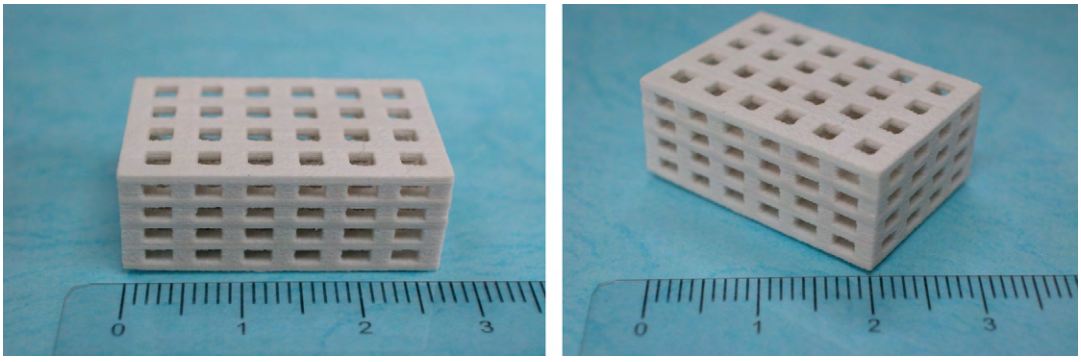

Fig. 12. A 3D reticular ceramic part made by selective laser gelling with inner channel structure and dimensions of 27 mm × 19 mm × 11 mm.

of support, the support will collapse because of the strength of joints in the support is weak.

Utilizing optimal process parameters for generating 100 μm thick layers, at a laser power of 15 W and scan velocity of 200 mm/s, we can demonstrate the ability of strategy for generating support to construct a reticular 3D ceramic part with an overhanging and inner channel structure as shown in Fig. 12. This part had a length of 27 mm, width of 19 mm, and a total height of 11 mm with 110 layers. The overhanging had the rectangular cross-section with dimensions of 1.5 mm × 1 mm, span of 2.5 mm, and a sagged deflection of 38.5 μm. Simultaneously, a multi-length support with dimensions of 0.2 mm × 0.3 mm × 1.5 mm was generated under the overhanging. Also, the total building time was 150 min, inclusive of paving slurry, generating support, and constructing ceramic body.

4. Discussion and conclusions

4.1. Suitable process parameters

If a complex and delicate object is desired to be fabricated, both the layer thickness and the value of surface roughness must be reduced. From Fig. 4 we know that when the gelled depth of a layer is thinner, the laser power decreases as the laser scan speed increases under the same laser power density. In this way, a more accurate part can be obtained, but the fabrication time must sharply increase because of the addition of a large number of building layers.

Figs. 7 and 8 show that the surface roughness and the dimensional accuracy of parts increase as the laser power decreases and that of parts decreases with the laser scan speed. In addition, the laser power density is proportional to the gelled depth. That is, raising the laser power or reducing the scan speed leads to an increase in the ceramic gelled depth. However, the surface roughness decreases as the gelled depth increases. In order to obtain a better surface roughness, a relatively lower laser power is needed. From Fig. 8 we can see that the specimen possesses an R_Z of 28 μm under a laser power of 9 W. The surface condition of this specimen is shown in Fig. 13.

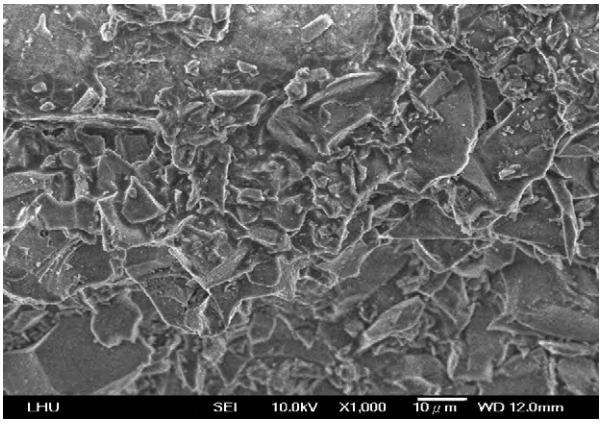

Fig. 13. SEM image of the surface of a ceramic specimen.

The generating strategy from the single line and single layer to the multi-layers ceramic was feasible and could be implemented in fabricating ceramic parts that could successfully be built within the parameter window: laser power (P_L) = 6–24 W, laser scan speed (V_s) = 50–350 mm/s, and layer thickness (L_t) = 0.05–0.1 mm. A set of suitable parameters was found to be: P_L = 15 W, V_s = 250 mm/s, L_t = 0.1 mm, overlap = 25%, over-gel = 30%, and the laser power density = 2.5 J/mm^3.

As the over-gel between each layer exceeds 50%, the accuracy of the part decreases due to the laser power density being too high. The over-gel below 10% is not practical because the bond between layers is insufficient. When the overlap is greater than 40%, the gelled layer gets warped. However, the gelled layer will be divided into several thin pieces during the scraping operation if the overlap is less than 15%.

4.2. The slurry material

The SLA, SLS, and 3DP utilizing scraper or roller to pave materials have two drawbacks that need to be solved: expensive raw materials and poor surface roughness. First, although a layer thickness below 50 μm is easy to build using SLA in the liquid state, SLA is not a popular process due to the expensive UV-resin. The monomers of the resin have a low storage lifetime, leading to a high cost of the precursor materials. Second, any kinds of powder-based materials can be formed by SLS or 3DP, but a more accurate layer is hardly to be paved because the smaller powder particle can easily be attached on the scraper and many voids are formed onto the surface of the paved layer. In addition, the surface finish quality of above two methods is constrained by the size of the powder.

To overcome these two problems, we propose a slurry-based material employed in SLG. The experimental results show that the formability of the slurry material outperforms the conventional method. The slurry reduces the attachment of particles on the bottom of the scraper to reduce the value of surface roughness of the paved layers. Furthermore, the slurry material is easily to be paved below a layer thickness of 50 μm that is similar to SLA with liquid-based materials, thus, it can enhance the dimensional accuracy. The slurry material maintains the advantages of SLA while eliminating the drawbacks of SLS and 3DP because the silica powder is very inexpensive and the silica slurry is easily to be paved into a thinner layer.

The silica powder and sol are mixed in a proportion of 50:50 to 60:40 wt.% to form the slurry. The rate of gelling appears to be proportional to the sol concentration. Adding more silica sol increases the gelling rate significantly and the formability of a gelled layer is more easy, but the amount of sagged deflection for generating the overhanging increases because the sol among the silica particles will keep the gelling process before the water being evaporated by the laser radiation. In order to reduce the deflection of layers, the proportion of the sol in the slurries ought to decrease. In contrast, when the sol rate is below 30 wt.%, the slurry layer is hardly to be paved due to the higher viscosity. Therefore, a suitable proportion of silica powder and silica sol is 55:45 wt.%, which forms the ceramic slurries with suitable viscosity to avoid precipitation.

4.3. The influence of support structure

As the layer-additive technologies are employed in RP systems, a support structure is necessary to be constructed to maintain the shape of the overhanging unchangeably except the presented RP processes, e.g., SLS, LOM, FDM, and 3DP, already have solid supports to provide resistance against downward deflection.[1,3,5] Many processes, e.g., SLA, Inkjet, and LOM, can only fabricate a ceramic part with outer complex-shape, but cannot fabricate a part with inner complex structure because of solid supports are hard to be removed completely.[16]

The silica materials in slurry form were used in this work, the support did not need to be built to avoid warping due to the silica suspensible effect. However, a longer overhanging portion could not be constructed without generating a support because the suspensible effect insufficient to maintain the weight of the overhanging, thus support structures were necessary to be constructed when build the complex geometric features such as undercuts, overhangs, and internal voids.

From the side-view of the specimen as shown in Fig. 10(a), we observe that the protrusion had an overhanging structure, the overhanging yielded greater deflection as soon as the rate of span-thickness exceeded 25. Therefore, the pillared silica support needed to be generated to maintain the overhanging and to avoid warping. In other words, when an additional support is built, resistance downward deflection is available. The supports had the rectangular cross-section with dimensions of 0.25 mm × 0.3 mm and a span of 1.5 mm, these supports could avoid overhang yielding deflection as the span-thickness rate less 20.

After the object had been built, both the pillared supports and the residual slurries un-gelled by laser were cleaned with water jet at a low pressure to yield a high fidelity pattern that accurately represented the CAD model without deforming, and then no further shaping processing was needed.

Acknowledgements

This work was supported by the College of Engineering in Lunghwa University of Science and Technology. We also gratefully acknowledge the financial support from the Ministry of Education of Taiwan under Contract 99M-88-067.

References

1. Huang YM, Jeng JY, Jiang CP. Increased accuracy by using dynamic finite element method in the constrain-surface stereolithography system. *Journal of Materials Processing Technology* 2003;**140**(1–3):191–6.
2. Regenfuss P, Streek A, Hartwiq L, Klotzer S, Brabant T, Horn M, et al. Principles of laser microsintering. *Rapid Prototyping Journal* 2007;**13**(4):204–12.
3. Bandyopadhyay A, Das K, Marusich J, Onaqoruwa S. Application of fused deposition in controlled microstructure metal–ceramic composites. *Rapid Prototyping Journal* 2006;**12**(3):121–8.
4. Ozkol E, Ebert J, Telle R. An experimental analysis of the influence of the ink properties on the drop formation for direct thermal inkjet printing of high solid content aqueous 3Y-TZP suspensions. *Journal of the European Ceramic Society* 2010;**30**:1669–78.
5. Chiu YY, Liao YS, Hou CC. Automatic fabrication for bridged laminated object manufacturing (LOM) process. *Journal of Materials Processing Technology* 2003;**140**(1–3):179–84.
6. Friedel T, Travitzky N, Niebling F, Scheffler M, Greil P. Fabrication of polymer derived ceramic parts by selective laser curing. *Journal of the European Ceramic Society* 2005;**25**:193–7.
7. Tang Y, Fuh JYH, Loh HT, Wong YS, Lu L. Direct laser sintering of a silica sand. *Materials and Design* 2003;**24**:623–9.
8. Liou FW, Ruan J. Rapid manufacturing research and development for high performance materials. In: *Proceedings of international conference on advanced manufacturing*. 2007. p. 15.
9. Van Der Eijk C, Aseb O, Mugaas T, Karlsen R, Skjevdal R, Boivie K. Metal printing process: a rapid manufacturing process based on xerography using metal powders. *Materials Science and Technology* 2005;**3**: 3–9.
10. Song JL, Li YT, Deng QL, Hu DJ. Rapid prototyping manufacturing of silica sand patterns based on selective laser sintering. *Journal of Materials Processing Technology* 2007;**187–188**:614–8.
11. Lu X, Lee Y, Yang S, Hao Y, Evans JRG, Parini CG. Sovent-based paste extrusion solid freeforming. *Journal of the European Ceramic Society* 2010;**30**:1–10.
12. Liu HC, Tsuru H, Cooper AG, Prinz FB. Rapid prototyping methods of silicon carbide microheat exchangers. *Journal of Engineering Manufacturing* 2005;**219**(7):525–38.
13. Liu FH, Liao YS. A rapid prototyping apparatus for forming ceramic part. *Key Engineering Materials* 2008;**364–366**:383–8.
14. Klocke F, McClung A, Ader C. Direct laser sintering of borosilicate glass. In: *Proceedings of solid freeform fabrication symposium*. 2004. p. 236.
15. Cai K, Guo D, Huang Y. Solid freeform fabrication of alumina ceramic parts through a lost mould method. *Journal of the European Ceramic Society* 2003;**23**(6):921–5.
16. Noguera R, Lejeune M, Chartier T. 3D fine scale ceramic components formed by ink-jet prototyping process. *Journal of the European Ceramic Society* 2005;**25**:2055–9.